

Design and Modelling of Acost Effective Ac Voltage Stabilizer with Fuzzy Control

K.Haritha & Ch.Srinivas

¹M.Tech, Student Scholar, EEE Dept., St. Martin's Engg. College, Dhullapally, Secunderabad, Telangana.

²AssociateProfessor, EEE Dept., St. Martin's Engineering College, Dhullapally, Secunderabad, Telangana.

ABSTRACT—*in this paper we are developing a novel proposes a AC voltage regulator is used in both the domestic and industrial sectors for protecting the system from undesired effects is due to random voltage variations of the power supply. The paper introduces an ac voltage stabilizer/converter (ACVS) that is based on aFLC controller technology. A fuzzy control system is a control system based on fuzzy logic—a mathematical system that analyzes analog input values in terms of logical variables that take on continuous values between 0 and 1, in contrast to classical or digital logic, which operates on discrete values of either 1 or 0.The main theme of this paper is ACVS offers a specified strategy of voltage regulation, less harmonics, and low cost. The paper explains the operating principle of the ACVS with fuzzy logic controller and derives its nonlinear mathematical model. To ensure the desired performance of the ACVS while it is subject to any undesireableinput voltage and load variations, an optimal fuzzy logic control strategy is designed. It is achieved via transforming the ACVS model extending with fictive axis emulation into a rotating reference frame and the linearization of the model via specific orientation of the reference frame and introducing a linear control action. Operation of the ACVS is simulated under different disturbances due to load and grid voltage changes, and compared to voltage stabilization with application of fuzzy controllers. Simulation results are presented to demonstrate the voltage regulation with fuzzy control technology.*

Index Terms—AC–AC power conversion, electric variables control, linear-quadratic control, power quality, voltage control, fuzzy control.

INTRODUCTION

In recent year we are facing various power quality issues like lighting dimming, loss of heat control, loss of optimal operation status, and loss of motor control . These problems not only decrease the efficiency of the equipment operation but also lead to an unwanted extra electrical energy consumption. Among those methods, a traditional transformer with power electronic controlled tap changers is reported recently . The transformer is connected in between the power supply and the sensitive load. Part of the secondary winding is mounted with several taps and hence the whole winding is divided into a few sections. This method has disadvantages which

limits its applications. In fact, the adjustment of the voltage level is not smooth and has to be step changes; the range of voltage regulation is relatively narrow ; and the compensation by tapchanging transformer is accomplished with a time delay since the thyristor-based switches can be turned ON only once per ac cycle .

With the advances of the high-speed power electronic switching devices, various topologies of power converters are proposed /developed to achieve controlled ac to ac conversion . Bidirectional switches, which normally have two switching devices connected in series and each switch is paralleled with a diode for bypass, are adopted in the circuit for ac to ac conversion .

Through the mathematical derivation and theoretical analysis, the original ACVS model is converted into a linear model in the control and state space, in which the control task is to stabilize the output voltage solution which resembles the proposed topology, is reported in for an ac single-phase dynamic voltage restorer. It is a combination of a transformer and a single-phase ac–ac matrix converter which not only regulates the voltage on the primarywinding but also allows the changing of its phase angle by 180°.

This paper develops a systematic voltage controller adopting a converter model-based approach, and rigorous design methods rooted from linear systems and the optimal control theory is applied to achieve predefined control quality. The approach proposed in this paper avoids sinusoidal reference tracking problem encountered and the drawbacks due to intuitive solutions reported . The main contributions of the paper present in the development of a whole ACVS dynamical mathematical model with systematically designed control and the improvement of the feedback control technology for singlephase voltage stabilizers that is different from the methods used .

Description Of The Acvs Circuit Topology And Its Operation Principles

The circuit diagram of the proposed ACVS is shown in Fig. 1. It can be seen that the voltage

stabilizer mainly consists of a transformer connected to form an autotransformer and four power electronic switches. The primary winding of the transformer is connected to the mains with the voltage v_{in} through a pair of pulse width modulation (PWM) controlled bidirectional

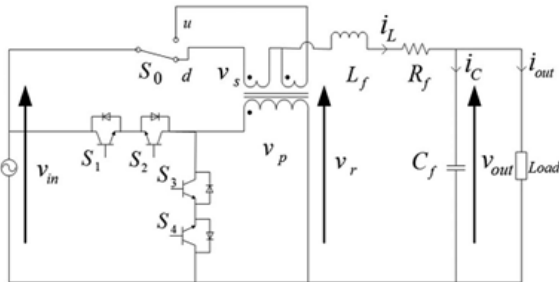


Fig. 1. Topology of the proposed ac voltage converter.

switches S1-S2. The switches S3-S4 are placed to provide a path for the primary winding energy dissipation to work with ON/OFF status changes of S1-S2. The “ON” and “OFF” status of the PWM control signal for the switches S3-S4 are complementary or opposite to the one applied to S1-S2. To avoid the overlapping of the two sets of switches, a delayed switching ON time is introduced. The transformer has two secondary windings which may have the same number of turns with polarity marks arranged as shown in Fig. 1 so the voltages of the two windings have an 180° phase shift

Step-Down Mode

When the voltage v_{in} is higher than the reference voltage, this mode is applicable. In this mode, S0 is switched to “d” position. The two pairs of switches S1/S2 and S3/S4 are switched ON and OFF with the PWM control. The primary winding voltage of the transformer is zero so $v_{out} = v_{in}$ approximately in this state. The PWM control gate signals for S1-S2 and S3-S4 are depicted in Fig. 2.

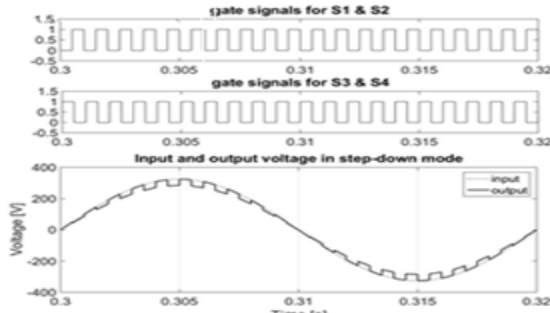


Fig. 2. Input and original output voltage without filtering comparison in step-down mode (duty ratio $D = 0.5$, switching frequency $f_s = 1$ kHz).

Step-Up Mode

The step-up operation mode is designed for the case when the input voltage is below the required output voltage. In this mode S0 is switched to “u” position. With the similar analysis conducted in the above section, the input and output voltages are shown in Fig. 3. The gate signals are the same as in Fig. 2.

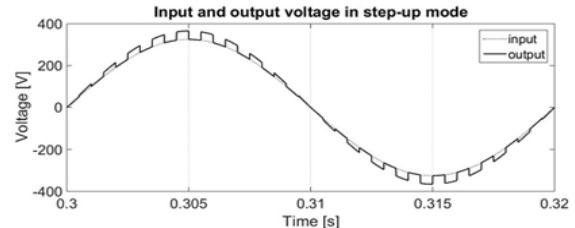


Fig. 3. Input and original output voltage without filtering comparison in step-up mode (duty ratio $D = 0.5$, switching frequency $f_s = 1$ kHz).

MODELING OF THE AC VOLTAGE STABILIZER

Model of the ACVS

The voltage on the primary winding of the transformer is controlled by the four switches, which can be described by

$$v_p(t) = v_{in}(t)g(t) \quad (1)$$

where v_p is the primary winding voltage and g is the gate switching function of S1-S2.

The relationship between the primary winding voltage and the secondary winding voltage is expressed as

$$\frac{v_s(t)}{v_p(t)} = \pm \frac{1}{k} \quad (2)$$

where v_s is the transformer secondary winding voltage, and the upper sign is for the step-up mode, whereas the lower sign is for the step-down mode.

The voltage before the filter v_r is

$$v_r(t) = v_{in}(t) + v_s(t) \quad (3)$$

The output voltage accounts the voltage across the inductor of the L-C filter

$$v_{out}(t) = v_r(t) - L_f \frac{di_L(t)}{dt} - i_L(t)R_f \quad (4)$$

where i_L is the inductor current, L_f and R_f are the inductance and the resistance of the filter inductor, respectively. The inductor current is

$$i_L(t) = i_C(t) + i_{out}(t) = C_f \frac{dv_{out}(t)}{dt} + i_{out}(t) \quad (5)$$

where i_C is the capacitor current, C_f is the capacitance of the filter capacitor, and i_{out} is the load current.

Substituting (1)-(3) and (5) into (4) yields

$$v_{out}(t) = v_{in}(t) \left[1 \pm \frac{g(t)}{k} \right] - \left[L_f C_f \frac{d^2 v_{out}(t)}{dt^2} + L_f di_{out}(t)dt + R_f C_f dv_{out}(t)dt + R_f i_{out}(t) \right] \quad (6)$$

Assume that the duty ratio $D(t)$ is fixed in a single switching period. Then, the gate switching function can be expressed as

$$g(t) = \begin{cases} 1 & nT_s < t < (n + D(t))T_s \\ 0 & (n + D(t))T_s < t < (n + 1)T_s \end{cases} \quad (7)$$

where $n = 0, 1, 2, 3, \dots$ represents the number of sample time. Applying Fourier series expansion to decompose (7), it can be obtained as follows [7]:

$$g(t) = D(t) \sum_{m=1}^{\infty} \frac{2 \sin(mD(t)\pi)}{m\pi} \cos(m\omega_s t) \quad (8)$$

where ω_s denotes the angular switching frequency.

According to (8), the switching function consists of the duty ratio and high-frequency harmonic components. Since the harmonics are filtered out by the L-C filter afterward, switching function $g(t)$ can be replaced by $D(t)$ approximately. Therefore, (6) can be rewritten as

$$v_{out}(t) = v_{in}(t) \left[1 \pm \frac{D(t)}{k} \right] - \left[L_f C_f \frac{d^2 v_{out}(t)}{dt^2} + L_f \frac{di_{out}(t)}{dt} + Rf C_f \frac{dv_{out}(t)}{dt} + Rf i_{out}(t) \right] \quad (9)$$

Equation (9) establishes the relationship between the input voltage, output voltage, and converter parameters with the load current as one of uncertain input variables, from which the following are noticed:

- 1) the output voltage is sinusoidal both in steady states and transients due to the input voltage being sinusoidal;
- 2) change of the magnitude of the input voltage v_{in} is a disturbance of the model;
- 3) another disturbance is the load current i_{out} which depends on the load type and it is unpredictable;
- 4) the control input is the duty ratio D which should be adjusted to keep the output voltage magnitude constant;
- 5) the control input is bounded between 0 and 1;
- 6) the model is nonlinear due to available sinusoidal input voltage and its product with the control action.

These features make the design of the output voltage magnitude controller a difficult task. However, a sufficient solution for low-cost implementation is found via nonstandard transformation of the model of the voltage converter.

Model Transformation

This section introduces a model transformation which converts the complex control design task of the sinusoidal ac voltage output magnitude into a linear control system design frame. The method is similar to the ac machines' two-phase description in an arbitrary rotating reference frame d-q instead of a stationary reference frame a-b [17]. A similar approach was adopted in [18] and applied to current loop control of a single-phase voltage-source

Then, (5) for the two-phase converter can be put into a vector forms

$$i_{Lab}(t) = C_f \frac{dv_{outab}(t)}{dt} + i_{outab}(t) \quad (10)$$

where $i_{Lab}(t) = [i_{La} \ i_{Lb}]^T$, $v_{outab}(t) = [v_{outa} \ v_{outb}]^T$, and $i_{outab}(t) = [i_{outa} \ i_{outb}]^T$.

Equation (4) with substitutions of (1)–(3) and accounting (8) is transformed to

$$v_{outab}(t) = v_{inab}(t) \left[1 \pm \frac{D(t)}{k} \right] - \left[L_f \frac{di_{Lab}(t)}{dt} - i_{Lab}(t) Rf \right] \quad (11)$$

where $v_{inab}(t) = [v_{ina} \ v_{inb}]^T$. Note that $D(t)$ is a scalar function and it is the control input for both "a" and "b" axes. The control splits into two elements of the vector below

$$v_{pab}(t) = v_{inab}(t) D(t) \quad (12)$$

where $v_{pab}(t) = [v_{pa} \ v_{pb}]^T$, and v_{pa}, v_{pb} denote the primary winding voltages in the real and fictive converters, respectively. A d-q orthogonal reference frame is introduced which is rotating with the velocity equal to the angular frequency ω of v_{out} . The angle between the d-q and a-b frames is θ and $d\theta/dt = \omega$. Fig. 4 shows an example of transformation for the inductor current vector.

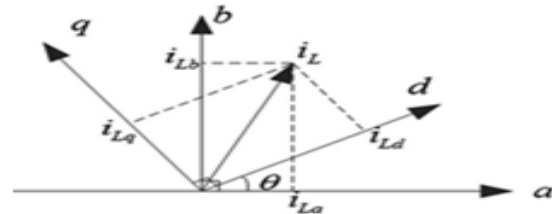


Fig. 4. Transformation of vectors from a-b to d-q reference frame

Mathematically, the transformation is described as

$$\begin{bmatrix} i_{Ld} \\ i_{Lq} \end{bmatrix} = \begin{bmatrix} \cos \theta & \sin \theta \\ -\sin \theta & \cos \theta \end{bmatrix} \begin{bmatrix} i_{La} \\ i_{Lb} \end{bmatrix} \quad (13)$$

A similar transformation applies for the rest of the vectors. In result, the elements of the vectors in the d-q frame are constants in steady states and not sinusoidal during transients, although the elements of the corresponding vectors in the a-b frame are sinusoidal.

Equations (10) and (11) in the d-q reference frame are obtained as

$$i_{Ldq}(t) = C_f \frac{dv_{outdq}(t)}{dt} + C_f \omega j v_{Ldq}(t) + i_{outdq}(t) \quad (14)$$

$$v_{outdq}(t) = v_{indq}(t) \left[1 \pm \frac{D(t)}{k} \right] - L_f \frac{di_{Ldq}(t)}{dt} - L_f \omega j i_{Ldq}(t) + i_{outdq}(t) \quad (15)$$

Where $v_{outdq}(t) = [v_{outd} \ v_{outq}]^T, i_{outdq}(t) = [i_{outd} \ i_{outq}]^T, i_{Ldq}(t) = [i_{Ld} \ i_{Lq}]^T, v_{indq}(t) = [v_{ind} \ v_{inq}]^T$, and $J = \begin{bmatrix} 0 & -1 \\ 1 & 0 \end{bmatrix}$.

It is noticed that additional terms (due to available time derivatives) depending on ω are introduced into the equations via the transformation. The corresponding equations for d- and q-axes are coupled in (14) and (15) due to J whereas the initial equations for a and b-axes in (10) and (11) are independent. The system of (14) and (15) can be organized in a state-space form as follows:

$$\dot{X} = AX + Bu + W \quad (16)$$

Align the d-q reference frame with the output voltage vector. Then,

$$v_{outd} = |v_{outdq}| = |v_{outab}| = |v_{out}| \quad (17)$$

where $|v_{out}|$ is the magnitude of the actual single-phase output voltage. Note that the magnitude of any vectors in the d-q and a-b reference frames is same.

The approach from [18] introduces a decoupling control making the d and q-axes equations independent. Inspired by the methodology, the paper proposes a new solution which is less complicated in control implementation and it is feasible in this case due to specific topology of the voltage stabilizer.

The second equation of (16) in the reference frame aligned with the output voltage vector gives the following algebraic equation for relating i_{Lq} to output voltage and current:

$$i_{Lq} = C_f w |v_{out}| + i_{outq} \quad (18)$$

From (18), i_{Lq} is not an independent variable so it can be eliminated from the third equation of (16). Then, the fourth equation of (16) gives dynamics of v_{inq}

$$v_{inq} = \frac{kL_f}{k+D(t)} \left[2wi_{Ld} + \frac{R_f C_f w}{L_f} |v_{out}| + \frac{R_f}{L_f} i_{outq} - wi_{outd} + di_{outqd}t \right] \quad (19)$$

The parameters of the filter are chosen in such a way to provide a negligible angle difference between the input and output voltage vectors of the ACVS, which results in $v_{inq} \approx 0$.

CONTROL STRATEGY

The goal of the control is to adjust automatically the duty ratio to stabilize the output voltage magnitude (or rms value) at the rated value $|v_{out}|^*$ in the presence of disturbances due to changes of the magnitude of the mains voltage and the voltage variations on the filter as the result of the load change. The paper proposes an alternative

approach introducing a new control input $u_2 = |v_{in}|D(t)$ which makes the model linear.

To obtain a zero steady-state control error, model (20) is augmented with an additional state coordinate as an integral of the voltage magnitude error and the corresponding equation

$$v_i = \int_0^t (|v_{out}| - |v_{out}|^*) dt \quad (20)$$

The quadratic cost function for system (22) is defined [19]

$$J = \int_0^\infty (X_2^T Q X_2 + u_2^T R u_2) dt \quad (21)$$

where Q and R are the matrices of positive symmetric weighting, expressed as diagonal matrices. The optimal control law with integral feedback is expressed as [20]–[22]

$$u_2 = -KX_2 \quad (22)$$

ACVS with d-q transformation and LQR control.

$$P A_2 + A_2^T P - P B_2 R^{-1} B_2^T + Q = 0 \quad (23)$$

Note that LQR feedback gains for the step up and step-down modes will be the same only with opposite signs. Due to this, the sign before reference in (21) depends on the operation mode, meaning that for the output voltage increase the duty ratio is increased in the step-up mode and it is reduced in the step-down mode.

The required for control duty ratio can be computed as

$$D(t) = u_2 / |v_{in}| \quad (24)$$

The block diagram of the proposed single-phase ACVS with d-q transformation and LQR control is depicted in Fig. 5.

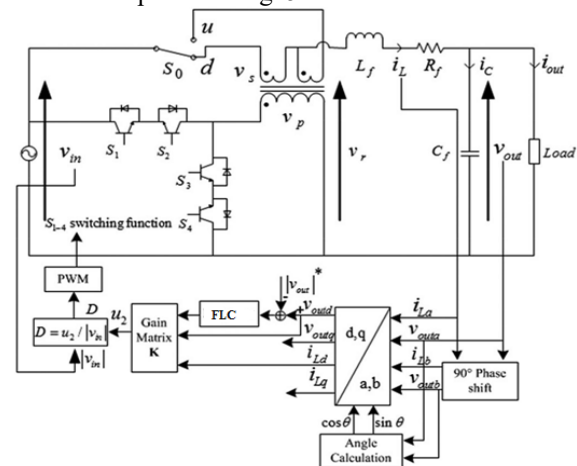


Fig. 5. Block diagram of the proposed single-phase

III. FUZZY LOGIC CONTROLLER

In FLC, basic control action is determined by a set of linguistic rules. These rules are determined by the system. Since the numerical variables are converted into linguistic variables,

mathematical modeling of the system is not required in FC.

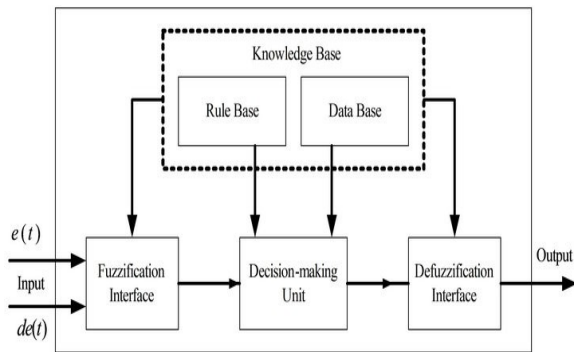


Fig.6.Fuzzy logic controller

The FLC comprises of three parts: fuzzification, inference engine and defuzzification. The FC is characterized as i. seven fuzzy sets for each input and output. ii. Triangular membership functions for simplicity. iii. Fuzzification using continuous universe of discourse. iv. Implication using Mamdani's, 'min' operator. v. Defuzzification using the height method.

TABLE I: Fuzzy Rules

| Change in error | Error | | | | | | |
|-----------------|-------|----|----|----|----|----|----|
| | NB | NM | NS | Z | PS | PM | PB |
| NB | PB | PB | PB | PM | PM | PS | Z |
| NM | PB | PB | PM | PM | PS | Z | Z |
| NS | PB | PM | PS | PS | Z | NM | NB |
| Z | PB | PM | PS | Z | NS | NM | NB |
| PS | PM | PS | Z | NS | NM | NB | NB |
| PM | PS | Z | NS | NM | NM | NB | NB |
| PB | Z | NS | NM | NM | NB | NB | NB |

Fuzzification: Membership function values are assigned to the linguistic variables, using seven fuzzy subsets: NB (Negative Big), NM (Negative Medium), NS (Negative Small), ZE (Zero), PS (Positive Small), PM (Positive Medium), and PB (Positive Big). The Partition of fuzzy subsets and the shape of membership CE(k) E(k) function adapt the shape up to appropriate system. The triangular shape of the membership function of this arrangement presumes that for any particular E(k) input there is only one dominant fuzzy subset. The input error for the FLC is given as

$$E(k) = \frac{P_{ph}(k) - P_{ph}(k-1)}{V_{ph}(k) - V_{ph}(k-1)} \quad (25)$$

$$CE(k) = E(k) - E(k-1) \quad (26)$$

Inference Method: Several composition methods such as Max-Min and Max-Dot have been proposed in the literature. In this paper Min method is used. The output membership function of each rule is

given by the minimum operator and maximum operator. Table 1 shows rule base of the FLC.

Defuzzification: As a plant usually requires a non-fuzzy value of control, a defuzzification stage is needed. To compute the output of the FLC, „height“ method is used and the FLC output modifies the control output. Further, the output of FLC controls the switch in the inverter. In UPQC, the active power, reactive power, terminal voltage of the line and capacitor voltage are required to be maintained. To achieve this, the membership functions of FC are: error, change in error and output

The set of FC rules are derived from

$$u = -[\alpha E + (1-\alpha)C] \quad (27)$$

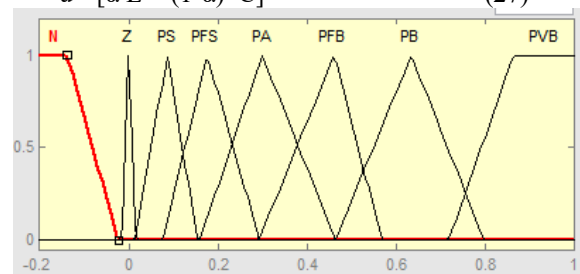


Fig 7 input error as membership functions

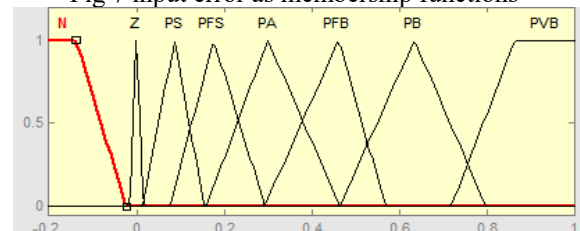


Fig 8 change as error membership functions

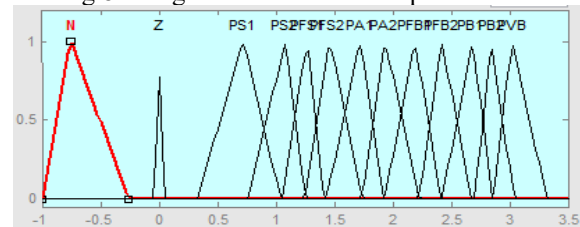


Fig.9 output variable Membership functions

Where α is self-adjustable factor which can regulate the whole operation. E is the error of the system, C is the change in error and u is the control variable.

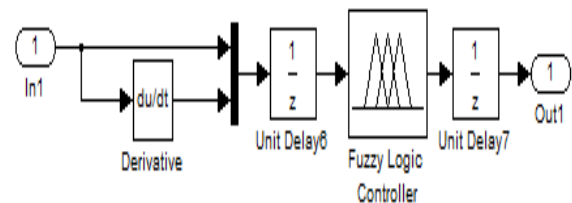


Fig 10.fuzzy logic controller in simulation
SIMULATION RESULTS

Fig :11 and 12 explain the simulation block and control diagram of the proposed AC voltage converter. The values of parameters are listed in Table I.

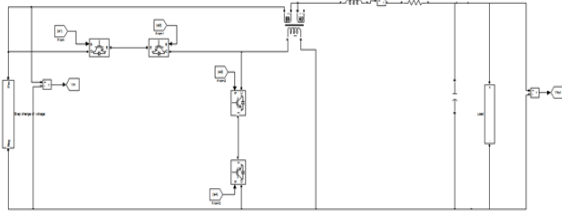


Fig:11 simulation block diagram of the proposed ac voltage converter.

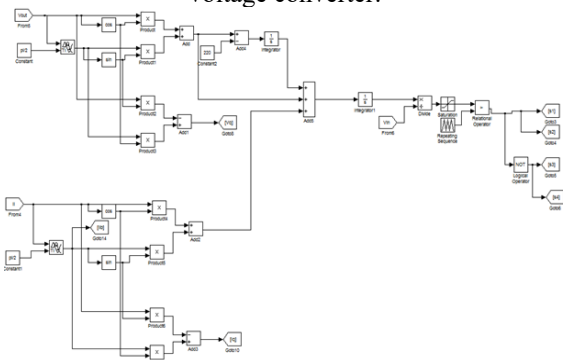


Fig :12 Control block diagram of the proposed ac voltage converter.

TABLE I
Circuit Parameters

| Parameter | Name | Value | Unit |
|---|---------------|--------------------------------------|---------------|
| Turn Ratio | k | 8 | - |
| Filter capacitance | C_f | 1 | μF |
| Filter inductance | L_f | 3.9 | mH |
| Filter resistance | R_f | 0.1 | Ω |
| Voltage frequency | f | 50 | Hz |
| Switching frequency | f_s | 20 | kHz |
| Referred output voltage magnitude (rms value) | $ V_{out} ^*$ | 310.2 (220) | V |
| Input voltage magnitude (rms value) | $ V_{in} $ | $310.2 \pm 10\%$ $(220 \pm 10\%)$ | V |
| Load current rms value | I_{out} | 0-10 | A |

Simulation Results of d-q Transformation

Comparison of the simulation results of the ACVS (without control) model (10), (11) in the a-b reference frame with model (16) in the d-q reference frame aligned with the output voltage vector according to (17)–(19), and with reduced order model (20) is shown in Figs. 13 and 14 for the step-down mode.

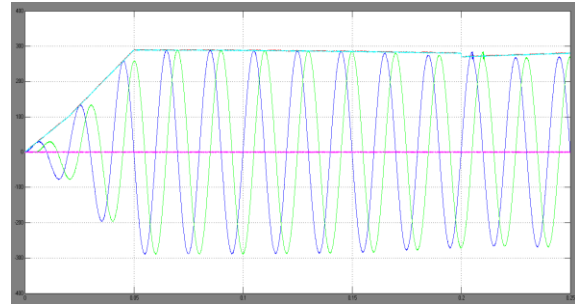


Fig. 13. Output voltages in the a-b and d-q reference frames.

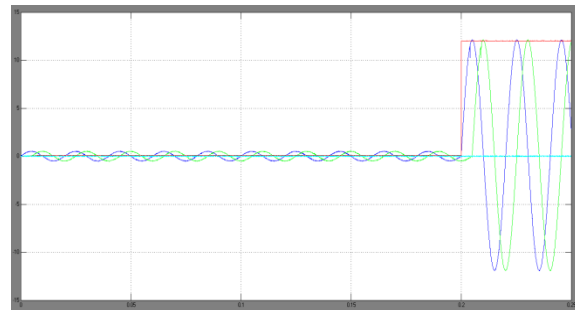


Fig. 14. Inductor currents in the a-b and d-q reference frames.

The state variables of model are marked with subscripts “original” and the variables of model (20) are denoted with subscripts “simplified.” From 0 to 0.05 s, the responses of the models to linear increase of the magnitude of the input voltage from 0 up to its rated value are simulated for the case of no load and constant duty ratio value of 0.3.

The difference between $v_{outd}.$ original and $v_{outd}.$ simplified is tiny (not exceeding 0.01%). Note that in steady state the first equation of model (16) gives $i_{Ld} = i_{outd}$ in the reference frame aligned with the output voltage vector. Thus, for the steady state with no load $i_{Ld} = 0$ while $i_{Lq} = 0$ explained by (18) as shown in the subplot of Fig. 12. The difference between $i_{Ld}.$ original and $i_{Ld}.$ simplified is also negligible (not bigger than 0.01%) validating the reduced order model for the control design purpose.

Simulation Results of Voltage Control With Different Loads

The results for instantaneous input and output voltages, and load currents are shown in Figs. 14, 15, and 16. They are also compared to the results obtained for the system when the LQR controller is replaced by fuzzy controllers with rms output voltage feedback instead of the voltage magnitude, and without d-q transformation.

Operation With Resistive Load: Fig. 8 shows that the distortion of the sinusoidal shape of the output voltage lasts for less than one-eighth of the period.

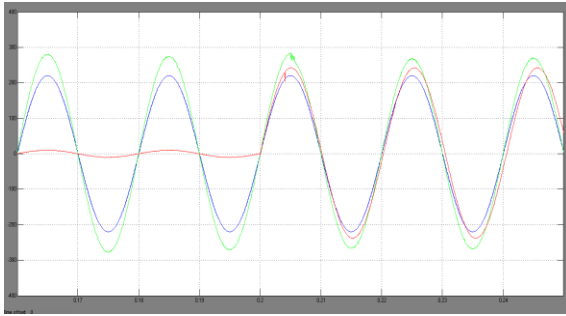


Fig. 15. Voltages and current instantaneous values After the engagement of the controllers, the output voltage rms values are gradually reduced to the reference value as 220 V.

The proposed LQR controller demonstrates the shortest settling time. After the load current increase at 0.2 s, the response overshoot of the system with fuzzy controller is much higher than in the cases of two other controllers.

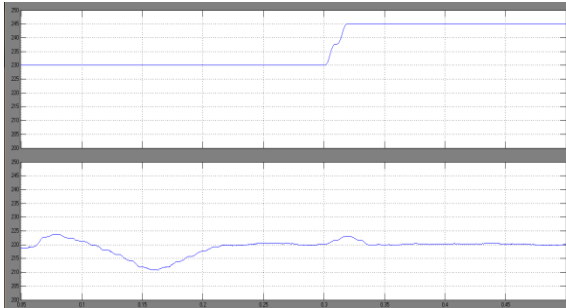


Fig. 16. Voltage rms values with step changed resistive load and input voltage increase.

Operation With Inductive Load: Fig. 16 shows that the distortions of the sinusoidal shape of the output voltage are less and shorter in this case than for the resistive load. As expected, there is a phase difference between the output voltage and current while the output voltage is still in phase with the input voltage.

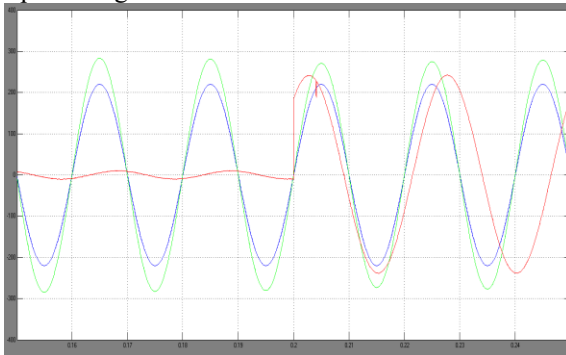


Fig. 17. Voltages and current instantaneous values with step changed inductive load
When the inductive load increases from 2.3 to 4.6 A at 0.2 s, the voltage starts to drop slightly

and then restores to the reference value with settling time 0.1 s, which is illustrated in the zoom-in view of Fig. 18. Fig. 18 also shows that the proposed LQR controller provides lower voltage overshoot and shorter settling time for both load and input voltage changes compared with PI and I controllers.

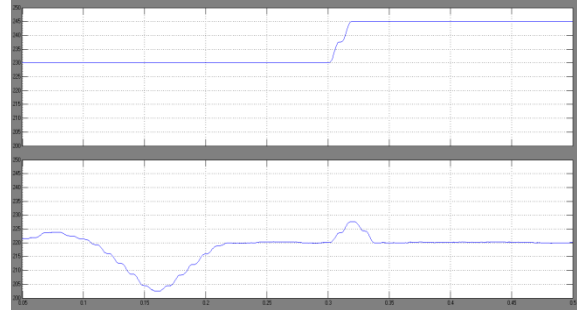


Fig. 18. Voltage and current rms values with step changed inductive load and input voltage increase.

Operation With Nonlinear Load: Although the load current is highly distorted, the output voltage (see Fig. 19) has a low harmonic distortion with 0.26% THD prior to the step load change at 0.2 s. After the current rises up, the THD increases to 1.64%. The simulation results in Fig. 18 demonstrate that the LQR controller gives the best performance among three controllers in terms of the settling time and overshoot.

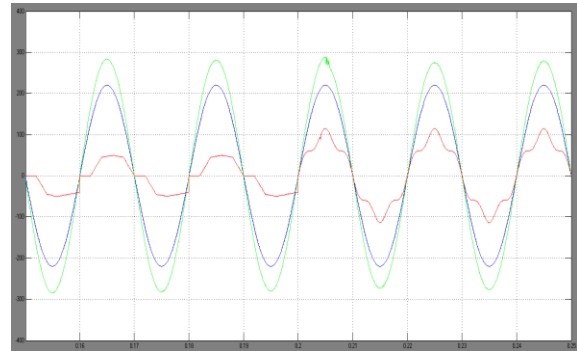


Fig. 19. Voltages and current instantaneous values with step changed nonlinear load.

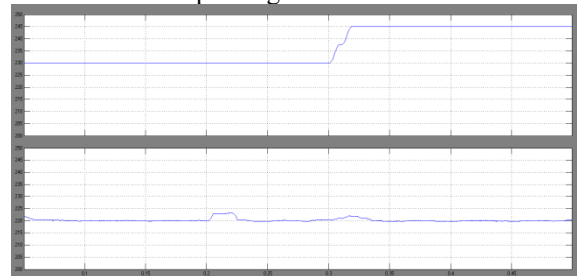


Fig. 20. Voltage and current rms values with step changed nonlinear load and input voltage increase.

CONCLUSION

The implementation of this paper with fuzzy control is for getting better for voltage regulation in uncertain conditions in the power system. For controlling the ACVS with fuzzy control, for providing the better voltage regulation, low harmonics and low cost. The working principle and the main characteristics of the ACVS with control are discussed. The mathematical model of the ACVS is developed and transformed into a d-q rotating reference frame to obtain a simplified model for the convenience of analysis. The simulation results convince that the full ACVS model and the simplified d-q frame model give the agreed responses, and performance of the d-q frame model provides a useful platform for the development and analysis of new robust controls to the ACVS for both the academic and industrial communities. So control strategies is very encouraging for improvement with disturbances from the both supply voltage and the load side variations.

REFERENCES

- [1] A. Felce, G. Matas, and Y. Da Silva, "Voltage sag analysis and solution for an industrial plant with embedded induction motors," in Proc. IEEE 39th Ind. Appl. Soc. Meet./Ind. Appl. Conf., 2004, vol. 4, pp. 2573–2578.
- [2] S. Z. Djokic, J. Desmet, G. Vanalme, J. V. Milanovic, and K. Stockman, "Sensitivity of personal computers to voltage sags and short interruptions," IEEE Trans. Power Del., vol. 20, no. 1, pp. 375–383, Jan. 2005.
- [3] A. Sannino, M. G. Miller, and M. H. J. Bollen, "Overview of voltage sag mitigation," in Proc. Power Eng. Soc. Winter Meet., 2000, vol. 4, pp. 2872–2878.
- [4] S. M. Bashi, "Microcontroller-based fast on-load semiconductor tap changer for small power transformer," J. Appl. Sci., vol. 5, no. 6, pp. 999–1003, 2005.
- [5] N. Yorino, M. Danyoshi, and M. Kitagawa, "Interaction among multiple controls in tap change under load transformers," IEEE Trans. Power Syst., vol. 12, no. 1, pp. 430–436, Feb. 1997.
- [6] Z. Jie, Z. Yunping, Y. Weifu, L. Lei, and L. Fen, "Research on AC chopper power module with module parallel control," in Proc. IEEE Appl. Power Electron. Conf. Expo., 2008, pp. 1324–1327. [7] B.-H. Kwon, B. D. Min, and J. H. Kim, "Novel topologies of AC choppers," IEE Proc. Electr. Power Appl., vol. 143, no. 4, pp. 323–330, 1996.
- [8] J. H. Kim, B. D. Min, B. H. Kwon, and S.C. Won, "A PWM buck-boost AC chopper solving the commutation problem," IEEE Trans Ind. Electron., vol. 45, no. 5, pp. 832–835, Oct. 1998.
- [9] J. P. Contreras, "Under-voltage and over-voltage AC regulator using AC/AC chopper," in Proc. IEEE Int. Symp. Ind. Electron., 2006, vol. 2, pp. 809–814.
- [10] N. Abd El-Latif Ahmed, K. Amei, and M. Sakui, "Improved circuit of AC choppers for single-phase systems," in Proc. Power Convers. Conf., 1997, vol. 2, pp. 907–912.



K.HARITHA

Completed B.Tech in Electrical & Electronics Engineering in 2013 from JNTU, HYDERABAD and Pursuing M.Tech from St. Martin's Engineering College, Dhullapally, Secunderabad, Telangana. Area of interest includes Power Electronics.

E-mail id: haritha.rupa@gmail.com



CH.SRINIVAS

Completed B.Tech in Electrical & Electronics engineering in 2006 from Dr. Palraj Engineering College, Badrachalam, Khammam Affiliated To Jntuh, Hyderabad University and M.E. in industrial drives and controls in 2010 from Osmania University, Working as Associate Professor in St. Martin's Engineering College, Dhullapally, Secunderabad, Area of interest includes industrial drives.

E-mail id: srinivas265@gmail.com